Response of microbial decomposition to spin-up explains CMIP5 soil carbon range until 2100

J.-F Exbrayat[1,2] A. J. Pitman[1] and G. Abramowitz[1]

[1]{ARC Centre of Excellence for Climate System Science and Climate Change Research Centre, University of New South Wales, Sydney, New South Wales, Australia}

[2]{School of GeoSciences and National Centre for Earth Observation, University of Edinburgh, Edinburgh, United Kingdom}

Correspondence to: J.-F. Exbrayat (j.exbrayat@ed.ac.uk)

Abstract

Soil carbon storage simulated by the Coupled Model Intercomparison Project (CMIP5) models varies 6-fold for the present day. Here, we confirm earlier work that this range already exists at the beginning of the CMIP5 historical simulations. We additionally show that this range is largely determined by the representation of microbial decomposition during each model's spin-up procedure from initialization to equilibration. The 6-fold range in soil carbon, once established prior to the beginning of the historical period (and prior to the beginning of a CMIP5 simulation), is then maintained through the present and to 2100 almost unchanged even under a strong business-as-usual emissions scenario. We therefore highlight that a commonly ignored part of CMIP5 analyses – the land surface state achieved through the spin-up procedure – can be important for determining future carbon storage and land surface fluxes. We identify the need to better constrain the outcome of the spin-up procedure as an important step in reducing uncertainty in both projected soil carbon and land surface fluxes in CMIP5 transient simulations.

1 Introduction

The land surface currently absorbs about a third of anthropogenic emissions of CO_2 (Canadell et al., 2007; Le Quéré et al., 2009) and so helps to offset global warming. Future global warming may enhance microbial decomposition and emissions of CO_2 from respired soil organic carbon (*SOC*), the largest carbon pool in the terrestrial biosphere (Jobbágy and Jackson, 2000). Higher

emissions from *SOC* could accelerate increases in atmospheric CO_2 concentrations even if plant carbon uptake by photosynthesis increased under higher atmospheric CO_2 (Ahlström et al., 2013; Friedlingstein et al., 2014; Nishina et al., 2014). Conversely, if the soil remains a carbon sink (Le Quéré et al., 2009; Lund et al., 2010) the negative feedback on rising atmospheric CO_2 (Davidson and Janssens, 2006) would help limit rates of increase. How soil carbon is represented in models and how it responds to climate is critical to resolving whether the land will remain a sink or become a source of CO_2.

Recent model intercomparisons, such as the fifth phase the Coupled Model Intercomparison Project (CMIP5; Taylor et al., 2012), or the Inter-Sectoral Impact Model Intercomparison Project (ISI-MIP; Warszawski et al., 2013) have highlighted a lack of consensus among models on whether the soil carbon sink will be sustained during the 21st century (Friedlingstein et al., 2014; Nishina et al., 2014). These models also exhibit large discrepancies in stores of *SOC* they simulate. For example, Todd-Brown et al. (2013) report that total *SOC* simulated by CMIP5 models for the present day represents a 6-fold variation ranging from ~510 to ~3040 Pg C. Another large range (~1090 to ~2645 Pg C) exists in the present day *SOC* simulated by ISI-MIP models despite being driven by a harmonized weather dataset (Nishina et al., 2014). These latter results indicate that a significant fraction of the uncertainty in estimates of total *SOC* arises from the representation of land processes rather than differences in climate drivers.

Soil carbon pools of widely different sizes have the potential to react differently to future climate change. We therefore examine the likely reasons for the large differences between CMIP5 models in their simulation of *SOC*. This work is founded in the recognition that the *SOC* varies among the CMIP5 models *for the present day* over a 6-fold range (Todd-Brown et al., 2013) and this range contributes to model-to-model variations in *SOC* change in the future (Todd-Brown et al., 2014). We explore *why* this 6-fold range exists and ultimately show that individual model responses to the spin-up procedure, particularly the dominant role of turnover time relative to *SOC* input, are the key reason for this range. Explaining why the amount of carbon mobilised in the active cycle varies greatly between models is critical but has been largely ignored in the literature to date. As noted by Knutti and Sedláček (2013), there may be multiple sources of disagreement between models such as a lack of process understanding, or the reduced availability of relevant observational datasets to constrain models. Technical aspects of climate modelling, such as how different state variables are initialized or spun up to an equilibrated state prior to an experiment being conducted, and how equilibration is defined in this context, can also lead to major differences between model simulations. Discriminating between these sources of

63 uncertainty to understand why CMIP5 models differ so significantly in the amount of *SOC* in the
64 present day, and subsequently in the total amount of C mobilized in the global cycle under a
65 future climate, enables an improvement in model projections. Increasing the consistency
66 between models is required to improve our confidence in the sign of the soil carbon feedback in
67 the future.

68

69 To avoid misconceptions, we define and differentiate between two states that are commonly
70 called "initial" states in land modelling. Our definition of "initial state", which is not known or
71 reported in CMIP5 models, is the state at the beginning of a climate model integration. This
72 "initial state" may come from a previous simulation, from off-line simulations, from
73 observations or via expert judgment. In the case of *SOC*, it may be initialized as a "cold start" or
74 in a state equilibrated with an atmosphere that reflects the period prior to the beginning of a
75 simulation. This model state is then commonly integrated forward in time until those model
76 states that are considered important are in equilibrium with the atmospheric model over some
77 period of time and to a degree that is defined by the modeller (but not reported). This generates
78 what we define as an "equilibrated state". In CMIP5, simulations are then reported from the
79 beginning of the historical period (say 1850), initialized with this "equilibrated state" and
80 integrated forward in time to the present day under observed forcings, and then into the future
81 using a representative concentration pathway (Taylor et al., 2012). The values of a climate
82 model's state variables at 1850 are commonly thought of as the "initial state" but they are not; it
83 is the model-specific equilibrated state under pre-industrial forcing and this reflects the skill of
84 the climate model to represent global and regional temperatures, rainfall and so forth. We
85 therefore call this the "equilibrated state" and note that this differs from the "initial state" due to
86 the Earth system model's simulated climate, the definition of "equilibrium" over time and space
87 and *crucially* how the state variables are parameterized. Here we show that a great deal of the 6-
88 fold range in *SOC* in the CMIP5 models at the "equilibrated state" assumed representative of
89 1850 (and consequently in the present day reported by Todd-Brown et al. (2013)) is a
90 consequence of the procedures used to evolve the model from the "initial state" to the
91 "equilibrated state". These procedures may influence how *SOC* changes through to 2100 (Todd-
92 Brown et al., 2014) due to the current state-of-the-art representation of *SOC* decomposition.

93

2 Material and methods

2.1 SOC in Earth System Models

In all global terrestrial models participating in recent intercomparison projects such as CMIP5 and ISI-MIP, the *SOC* balance and its change (ΔSOC) are represented in a similar way. First, inputs of carbon into the soil are derived from plant pools. Plant carbon uptake and turnover times respond to climate change, climate variability and atmospheric CO_2 independent of the size of the *SOC* pools. Meanwhile, modeled microbial decomposition releases carbon by heterotrophic respiration (R_h). The balance can be summarized by

$$\Delta SOC = SOC_{in} - R_h \quad (1)$$

where SOC_{in} is the input to the SOC pools from plant and litter pools.

Microbial decomposition is commonly represented as a first-order process and applied to a succession of pools. In each pool, a parameter k reflects the specific baseline decomposition rate (Xia et al., 2013; Exbrayat et al., 2013a,b) at a reference soil temperature and non-limiting moisture conditions. Then, the decay rate is adjusted at each time step by an environmental scalar (Todd-Brown et al., 2013; Xia et al., 2013; Exbrayat et al., 2013a,b; Nishina et al., 2014) that describes the instantaneous response of microbial activity to the soil physical state as the product of a soil temperature (f_T) and a soil moisture respiration function (f_W). Various formulations of f_T and f_W have been implemented in model codes (Lloyd and Taylor, 1994; Falloon et al., 2011; Todd-Brown et al., 2013; Exbrayat et al., 2013a,b; Nishina et al., 2014) usually assuming a space and time-invariant response to the same conditions. Their effect on decay rate varies according to local soil conditions and therefore climate.

The actual decay rate ($k \times f_T \times f_W$) is applied to the amount of substrate available, *SOC*, to determine the amount of microbial decomposition D_m at each model time step:

$$D_m = k \times f_T \times f_W \times SOC \quad (2)$$

where $k \times f_T \times f_W$ is equivalent to the fraction of respired substrate, the inverse of the turnover time SOC/R_h. A part of the decomposed organic matter is routed to pools with longer turnover time and the rest is emitted as CO_2. There may be variations between models in the number of pools they represent (Todd-Brown et al., 2013; Nishina et al., 2014) and the formulations of the environmental response functions (Falloon et al., 2011; Exbrayat et al., 2013a) but at the ecosystem scale, R_h is proportional to the amount of substrate, i.e. *SOC*, available in the soil.

This parameterization may be inconsistent with our current understanding of microbial decomposition (Allison et al., 2010; Schmidt et al., 2011; Wieder et al., 2013) because it lacks the representation of processes like microbial activity and priming effect (e.g. Xenakis and Williams, 2014). However, the first-order dependency of R_h on *SOC*, soil temperature and moisture is able to explain complex phenomenon like the apparent acclimation of decomposers to warming by quick depletion of the most labile substrate pools (Luo et al., 2001; Kirschbaum, 2004; Knorr et al., 2005).

2.2 CMIP5 data

From the CMIP5 archive we downloaded monthly soil carbon density (*cSoil* in metadata), litter carbon density (*cLitter*) and heterotrophic respiration (*rh*) for 15 CMIP5 models from 10 international institutions. A list of models can be found in Table 1 while further details about models and land components have been summarized in Table 2. We note that four of these models, namely BCC-CSM1.1 (model A), CCSM4 (model C), NorESM1-M and NorESM1-ME (grouped as model J), represent nitrogen limitation on plant productivity while the others do not. We selected data for the historical (1850-2005) and the most intensive Representative Concentration Pathway 8.5 (RCP 8.5, 2006-2100) experiments. A total of 79 simulations for the historical experiment, including 34 simulations continuing for RCP 8.5 (Table 1) were available. When *cLitter* was reported, we added it to *cSoil* as both pools are parameterized to generate R_h following first-order kinetics.

To calculate stock sizes we first multiplied spatially explicit data of *cSoil* and *cLitter* in kg C m^{-2} by corresponding grid-cell areas (*areacella* in metadata) and integrated their values globally. Similarly, we calculated global fluxes of R_h by multiplying monthly fluxes in kg C m^{-2} by grid-cell areas and integrating them globally. Fluxes were summed to obtain annual averages. Annual soil carbon input (SOC_{in}) from above ground biomass was not available from the database. Therefore, we calculated it by inverting the *SOC* balance:

$$SOC_{in} = \Delta SOC + R_h \quad (3)$$

As models did not start their historical simulations at the same time, we focus our analyses on the overlapping period of 1861-2100. We also averaged all simulations from the same model or

institution in an attempt to account for model dependence (see Bishop and Abramowitz, 2013, for a discussion on the topic).

In the following, we report values of stocks and fluxes averaged for three periods of time, the pre-industrial (1861-1870), modern (1996-2005) and future (2091-2100) periods. While the period 1861-1870 is not part of the pre-industrial control runs *sensu stricto*, the minor increase in atmospheric CO_2 between pre-industrial times (i.e. before 1850) and 1870 is unlikely to have led models to simulate a strong change in the greenhouse effect and terrestrial C fluxes. Values are shown in Table 3.

2.3 Harmonized World Soil Database

HWSD (FAO, 2012) is a global dataset of dominant soil units at a 30 second arc resolution, providing soil properties for the top (0-30 cm) and sub-soil (30-100 cm). We use version 1.21 and follow the approach by Todd-Brown et al. (2013) to obtain global values. First, we regridded the HWSD by selecting dominant soil units in a 0.5° latitude × 0.5° longitude grid. Then, we multiply the organic carbon content of the dominant soil units (in % weight) by the bulk density (provided in kg dm^{-3}) to obtain the carbon density (in kg C m^{-2}) in each 0.5° × 0.5° grid cell. We multiply the density by the surface area of each grid cell and sum results to obtain a total soil carbon content of ~1170 Pg C. Following Todd-Brown et al. (2013), a confidence interval of 29% below the mean (i.e. ~830 Pg C) to 32% above the mean (i.e. ~1550 Pg C) was considered to take variations in soil carbon content and the mapping processes into account. The range we obtain is slightly smaller than reported by Todd-Brown et al. (2013) (890 – 1660 Pg C) because we use an updated version of the HWSD and did not replace bulk density values for Andisols and Histosols.

3 Results

We first compare total *SOC* for pre-industrial (1861-1870), modern (1996-2005) and future (2091-2100) periods. Figure 1 compares the total *SOC* range in CMIP5 models for 1861-1870 (563 – 2938 Pg C), 1996-2005 (576 – 3047 Pg C), and 2096-2100 (582 – 3266 Pg C, derived using the RCP 8.5 scenario). All three periods show very similar distributions of *SOC* among the models and the present day and future ranges already exist at the beginning of the historical simulations. Figure 1 highlights that the size of SOC pools of individual CMIP5 models remain

largely consistent over the three time periods. Indeed, pre-industrial *SOC* predicts modern *SOC*, modern *SOC* predicts future *SOC* and pre-industrial *SOC* predicts future stocks with a high degree of precision (Figure 1). Also represented in Figure 1 is the 95% confidence interval of total *SOC* estimated from HWSD that we use as a reference for modern total *SOC* (i.e. in 1996-2005). We note that only three models fall within this range: BCC-CSM1.1 (model A), CanESM2 (model B) and HadGEM2 (model F). Models based on the CLM4 land surface model (i.e. models C and J) underestimate modern *SOC* while all remaining models overestimate it. Note that these models C and J include nitrogen limitation of the vegetation response to increasing CO_2.

We next investigate the likely reasons for the existence of this pre-industrial CMIP5 range in total *SOC*. The first obvious step is to check whether models are at equilibrium prior to and climate change experiments. Models may not agree on total *SOC* simply because some of them, and especially those at the extremes of the CMIP5 spectrum, are still drifting toward their own steady-state and therefore do not comply with our experiment protocol. In Figure 2 we show the relationship between pre-industrial SOC_{in} and R_h. This relationship is highly significant ($R^2 = 1$; $p < 0.001$) and strongly suggests that all models were equilibrated under pre-industrial boundary conditions. This removes the possibility that models were not in equlibrium and means that the 6-fold CMIP5 range is likely linked with the internal terrestrial processes represented in these models.

Two major internal terrestrial processes are involved: SOC_{in}, the amount of *SOC* that enters the soil pools, and the turnover time of organic matter that corresponds to the amount of *SOC* that is released from soil pools. The relationship between SOC_{in} and total *SOC* during the pre-industrial period is shown in Figure 3. Overall, the relationship is not significant (R^2=0.04; p=0.604). Further, the models that equilibrate with the largest total *SOC* stock (models E, H, I) are not the models with the largest *SOC* input. Similarly, the small equilibrated *SOC* pool size of models C and J seems unrelated to SOC_{in} despite these models including N limitations on plant productivity and SOC_{in}. In short, the amount of SOC_{in} cannot explain the size of the equilibrated pools. In Figure 4, we therefore present the relationship between the pre-industrial *SOC* turnover time (i.e. the inverse of the decay rate expressed as SOC/R_h) and total *SOC*. This relationship is highly significant ($p < 0.001$) and linear (R^2=0.84) and models with a longer turnover time, i.e. a low decay rate, require larger pools to offset the same *SOC* input, and vice-versa. Further, turnover times are not affected by the number of *SOC* pools represented. Models with the

longest turnover time have alternatively 9 (model E) or 2 pools (models H and I), while models with the shortest turnover time have 8 (model A), 6 (models C and J) or 4 pools (model F).

4 Discussion

Despite the change imposed on boundary conditions during global warming experiments (Anav et al., 2013; Friedlingstein et al., 2014), CMIP5 present day and projected *SOC* stocks are largely determined by their equilibrated pool size (Figure 1) in 1860. This was not unexpected due to the slow response of *SOC* pools but it clearly shows that modern and future stocks are mostly defined by the equilibrated pool size while changes can be explained by a combination of changes in the input and output fluxes (see Todd-Brown et al., 2014 for a detailed account of these mechanisms). Further, as *SOC* in 1860 is unknown from observations, CMIP5 models use a spin-up procedure from an initial state assuming steady pre-industrial boundary conditions (Xia et al., 2012) to obtain an equilibrated state for pre-industrial *SOC*. In order to reach equilibrium, iterative or semi-analytical methods (e.g. Xia et al., 2012) are employed to reach the pool sizes required to balance input (SOC_{in}) and output fluxes (R_h). Steady-state is assumed when the trend in ΔSOC becomes negligible. Hence, it is not the actual value of *SOC* that defines the equilibrium but its lack of variation in time (Xia et al., 2013; Exbrayat et al., 2013b). It is worrisome that these procedures are not clearly documented and therefore how a model is evolved from its true "initial state" to its "equilibrated state" is not known.

However, we have verified that all CMIP5 models were close to equilibrium prior to the initiation of climate change experiments. Following Equations 1 and 2, the model-specific value of *SOC* obtained by a model via spin-up depends on two factors. First, if SOC_{in} is large, a larger *SOC* pool is required to offset it through microbial decomposition and R_h, for a given decay rate, $k \times f_T \times f_W$. Conversely, low values of SOC_{in} lead *SOC* pools to equilibrate to lower values for a particular decay rate. Second, if the decay rate is high (short turnover time) during spin-up, *SOC* pools will remain small, for a given SOC_{in}. Conversely, low decay rates, or long turnover time, will require large pools of substrate to offset the same input SOC_{in}. Both factors are model-specific: SOC_{in} is derived from plant primary productivity fluxes (Davidson and Janssens, 2006) while the baseline decomposition rate k and the shape of the response functions f_T and f_W are highly model-dependent (Falloon et al., 2011; Exbrayat et al., 2013a,b; Todd-Brown et al., 2013).

Here we have shown that the large range exhibited by CMIP5 *SOC* is principally due to the response of microbial decomposition during the spin-up process. This is a long process that corresponds to multiple centuries of steady climate conditions but as noted is not reported as part of CMIP5 and might represent a short period if the "initial state" is already well equilibrated or may represent many centuries if not. Throughout this period however, for each CMIP5 model, model-specific parameter k and environmental response functions f_T and f_W drive *SOC* pools to the size required by the turnover time they simulate to compensate for SOC_{in}. This observation corroborates the predominance of turnover time in the uncertainty of ecosystem response to climate change (Friend et al., 2014) and Figure 4 shows that it is independent from the number of pools considered in each model. The resulting equilibrated state obtained *prior* to the initiation of CMIP5 transient simulations propagates through the present and into the future even when using RCP 8.5.

Our results raise a critical problem linked to model initialization and then equilibration by spin-up. According to our analysis of the CMIP5 models, a simple solution to reduce the uncertainty in simulated *SOC* stocks would be to modify model parameters, especially those related to *SOC* turn-over, to obtain a steady-state consistent from model to model with *SOC* values representative of pre-industrial conditions. Alternatively, because of the millennial time-scales of soil genesis, as well as land use changes, steady-state of global *SOC* stocks is not guaranteed to have existed at the end of the pre-industrial era. Therefore, one could choose to only consider model parameters that achieve modern stocks in accordance with observations in response to past changes (e.g. Exbrayat et al., 2014). However, this would require multiple realisations of computationally expensive models, or the use of emulators. Furthermore, it would be necessary to represent site history, and especially disturbances, with a high degree of confidence during simulations to avoid over-fitting parameters and this may not be realistic at global scale. Therefore, assuming an equilibrated pre-industrial state is a more readily available option that is supported by the lack of variations in simulated *SOC* during historical experiments despite changing boundary conditions. Thus, we suggest that one could use available estimates and confidence interval of modern *SOC* stocks to constrain the pre-industrial equilibrated state. These estimates include global datasets such as HWSD and other (Shangguan et al., 2014) but also regional data that may better represent high latitude stocks and permafrost (e.g. Northern Circumpolar Soil Carbon Database; Hugelius et al., 2013). Of course, while changing parameter values corresponding to *SOC* turnover time is relatively straightforward, it would be important to ensure that these pools are sustained by an input representative of carbon uptake. At equilibrium

281 SOC_{in} equals net primary productivity (NPP) because plant pools do not vary in size. Here all
282 models predict SOC_{in} within two standard deviations of the uncertainty range of modern, high
283 confidence, NPP estimates (56.4 ± 8–9 Pg C yr^{-1}; Ito et al., 2011). Although not directly
284 comparable with pre-industrial values, this global estimate indicates that models simulate
285 acceptable values of global carbon uptake.

286 As decomposition processes are represented following first-order kinetics, simulating more
287 realistic *SOC* stocks from an initial condition, and through spin-up to an equilibrated state in
288 response to adequate uptake fluxes would likely lead models to represent more correct modern
289 stocks. Nevertheless, as each model relies on its own formulation of the response functions f_T
290 and f_W, the ensemble would still exhibit different sensitivities of *SOC* stocks to climate change.
291 However, by removing a degree of freedom associated with spin-up procedures, we believe that
292 these observational datasets are a valuable tool for increasing the consistency between models
293 and making them more comparable. It would improve the confidence we can have in projections
294 of *SOC* fluxes and feedbacks on future climate change.

295

296 ## 5 Conclusions

297 We have demonstrated that the 6-fold range in *SOC* stocks simulated by CMIP5 models can be
298 explained by the model-specific response of microbial decomposition to spin-up under pre-
299 industrial conditions. Model dependent parameter and response functions drive the size of the
300 pools to the amount required by decay rates to offset SOC_{in} under the steady-state assumption.
301 Once established, the resulting pool sizes remain similar through to the present and into the
302 future even under the high-emissions RCP8.5 scenario that generates future conditions the least
303 similar to current ones. We therefore identify the spin-up procedure, and especially the response
304 of microbial decomposition during this very long model integration, as a key source of
305 uncertainty in the simulation of *SOC* in CMIP5 models. Critically, this involves the interaction
306 of a technical and a process-linked uncertainty in CMIP5 models' experimental framework. The
307 technical methods used for spin-up are model specific and not commonly reported. Interlinked
308 with the technical uncertainty is the parameterization of processes within the spin-up period.

309 A model that equilibrates to a soil carbon store well outside the observed range should be
310 examined with care. A very large amount of stored carbon increases the potential for the land
311 surface to become a source as even a tiny relative change in decay rate can strongly enhance R_h
312 and possibly reach a tipping point where it offset increases in SOC_{in}. Conversely, a very small

313 *SOC* store increases the likelihood that it will remain a sink. Such results are likely to be
314 artefacts of model implementation when *SOC* values are largely inconsistent with observed
315 ranges.

316 In conclusion, we recommend that future intercomparisons should constrain model parameters
317 so that each model achieves an equilibrated state similar to observations as the outcome of the
318 spin-up procedure. This would remove a degree of freedom associated with the process linking
319 initialization to equilibration via a poorly constrained spin-up procedure when comparing
320 differences in projected changes.

321

322 **Acknowledgements**

323 This work was supported by the Australian Research Council through grants DP110102618 and
324 CE110001028. We thank P. Petrelli for the availability of CMIP5 data and the National
325 Computational Infrastructure for data hosting and computational resources to process these
326 model data. We thank Dr K. Todd-Brown for guidance in processing the HWSD database and
327 Dr Y. Zhang for information about the BCC-CSM1.1 model.

328 We acknowledge the World Climate Research Programme's Working Group on Coupled
329 Modelling, which is responsible for CMIP, and we thank the climate modeling groups (listed in
330 Table 1 of this paper) for producing and making available their model output. For CMIP the U.S.
331 Department of Energy's Program for Climate Model Diagnosis and Intercomparison provides
332 coordinating support and led development of software infrastructure in partnership with the
333 Global Organization for Earth System Science Portals.

334

335 **References**

336 Ahlström, A., Smith, B., Lindström, J., Rummukainen, M. and Uvo, C. B.: GCM characteristics
337 explain the majority of uncertainty in projected 21st century terrestrial ecosystem carbon
338 balance, Biogeosciences, 10(3), 1517–1528, doi:10.5194/bg-10-1517-2013, 2013.

339 Allison, S. D., Wallenstein, M. D. and Bradford, M. A.: Soil-carbon response to warming
340 dependent on microbial physiology, Nat. Geosci., 3(5), 336–340, doi:10.1038/ngeo846, 2010.

341 Anav, A., Friedlingstein, P., Kidston, M., Bopp, L., Ciais, P., Cox, P., Jones, C., Jung, M.,
342 Myneni, R. and Zhu, Z.: Evaluating the Land and Ocean Components of the Global Carbon

343 Cycle in the CMIP5 Earth System Models, J. Clim., 26(18), 6801–6843, doi:10.1175/JCLI-D-
344 12-00417.1, 2013.

345 Arora, V. K. and Boer, G. J.: Uncertainties in the 20th century carbon budget associated with
346 land use change, Glob. Chang. Biol., 16(12), 3327–3348, doi:10.1111/j.1365-
347 2486.2010.02202.x, 2010.

348 Bentsen, M., Bethke, I., Debernard, J. B., Iversen, T., Kirkevåg, A., Seland, Ø., Drange, H.,
349 Roelandt, C., Seierstad, I. A., Hoose, C. and Kristjánsson, J. E.: The Norwegian Earth System
350 Model, NorESM1-M – Part 1: Description and basic evaluation of the physical climate, Geosci.
351 Model Dev., 6(3), 687–720, doi:10.5194/gmd-6-687-2013, 2013.

352 Bishop, C. H. and Abramowitz, G.: Climate model dependence and the replicate Earth paradigm,
353 Clim. Dyn., 41(3-4), 885–900, doi:10.1007/s00382-012-1610-y, 2012.

354 Canadell, J. G., Le Quéré, C., Raupach, M. R., Field, C. B., Buitenhuis, E. T., Ciais, P., Conway,
355 T. J., Gillett, N. P., Houghton, R. A. and Marland, G.: Contributions to accelerating atmospheric
356 CO2 growth from economic activity, carbon intensity, and efficiency of natural sinks., Proc.
357 Natl. Acad. Sci. U. S. A., 104(47), 18866–70, doi:10.1073/pnas.0702737104, 2007.

358 Chylek, P., Li, J., Dubey, M. K., Wang, M. and Lesins, G.: Observed and model simulated 20th
359 century Arctic temperature variability: Canadian Earth System Model CanESM2, Atmos. Chem.
360 Phys. Discuss., 11(8), 22893–22907, doi:10.5194/acpd-11-22893-2011, 2011.

361 Clark, D. B., Mercado, L. M., Sitch, S., Jones, C. D., Gedney, N., Best, M. J., Pryor, M.,
362 Rooney, G. G., Essery, R. L. H., Blyth, E., Boucher, O., Harding, R. J., Huntingford, C. and
363 Cox, P. M.: The Joint UK Land Environment Simulator (JULES), model description – Part 2:
364 Carbon fluxes and vegetation dynamics, Geosci. Model Dev., 4(3), 701–722, doi:10.5194/gmd-
365 4-701-2011, 2011.

366 Collins, W. J., Bellouin, N., Doutriaux-Boucher, M., Gedney, N., Halloran, P., Hinton, T.,
367 Hughes, J., Jones, C. D., Joshi, M., Liddicoat, S., Martin, G., O'Connor, F., Rae, J., Senior, C.,
368 Sitch, S., Totterdell, I., Wiltshire, A. and Woodward, S.: Development and evaluation of an
369 Earth-System model – HadGEM2, Geosci. Model Dev., 4(4), 1051–1075, doi:10.5194/gmd-4-
370 1051-2011, 2011.

371 Cox, P. M.: Description of the TRIFFID dynamic global vegetation model, Met Office Hadley
372 Centre Tech. Note, 24, 17pp, 2001.

373 Davidson, E. A. and Janssens, I. A.: Temperature sensitivity of soil carbon decomposition and
374 feedbacks to climate change, Nature, 440(7081), 165–173, doi:10.1038/nature04514, 2006.

375 Doney, S. C., Lindsay, K., Fung, I. and John, J.: Natural Variability in a Stable, 1000-Yr Global
376 Coupled Climate–Carbon Cycle Simulation, J. Clim., 19(13), 3033–3054,
377 doi:10.1175/JCLI3783.1, 2006.

378 Dufresne, J.-L., Foujols, M.-A., Denvil, S., Caubel, A., Marti, O., Aumont, O., Balkanski, Y.,
379 Bekki, S., Bellenger, H., Benshila, R., Bony, S., Bopp, L., Braconnot, P., Brockmann, P.,
380 Cadule, P., Cheruy, F., Codron, F., Cozic, A., Cugnet, D., Noblet, N., Duvel, J.-P., Ethé, C.,
381 Fairhead, L., Fichefet, T., Flavoni, S., Friedlingstein, P., Grandpeix, J.-Y., Guez, L., Guilyardi,
382 E., Hauglustaine, D., Hourdin, F., Idelkadi, A., Ghattas, J., Joussaume, S., Kageyama, M.,
383 Krinner, G., Labetoulle, S., Lahellec, A., Lefebvre, M.-P., Lefevre, F., Levy, C., Li, Z. X.,
384 Lloyd, J., Lott, F., Madec, G., Mancip, M., Marchand, M., Masson, S., Meurdesoif, Y., Mignot,
385 J., Musat, I., Parouty, S., Polcher, J., Rio, C., Schulz, M., Swingedouw, D., Szopa, S., Talandier,
386 C., Terray, P., Viovy, N. and Vuichard, N.: Climate change projections using the IPSL-CM5
387 Earth System Model: from CMIP3 to CMIP5, Clim. Dyn., 40(9-10), 2123–2165,
388 doi:10.1007/s00382-012-1636-1, 2013.

389 Dunne, J. P., John, J. G., Adcroft, A. J., Griffies, S. M., Hallberg, R. W., Shevliakova, E.,
390 Stouffer, R. J., Cooke, W., Dunne, K. A., Harrison, M. J., Krasting, J. P., Malyshev, S. L., Milly,
391 P. C. D., Phillipps, P. J., Sentman, L. T., Samuels, B. L., Spelman, M. J., Winton, M.,
392 Wittenberg, A. T. and Zadeh, N.: GFDL's ESM2 Global Coupled Climate–Carbon Earth System
393 Models. Part I: Physical Formulation and Baseline Simulation Characteristics, J. Clim., 25(19),
394 6646–6665, doi:10.1175/JCLI-D-11-00560.1, 2012.

395 Exbrayat, J.-F., Pitman, A. J., Abramowitz, G. and Wang, Y.-P.: Sensitivity of net ecosystem
396 exchange and heterotrophic respiration to parameterization uncertainty, J. Geophys. Res.
397 Atmos., 118(4), 1640–1651, doi:10.1029/2012JD018122, 2013a.

398 Exbrayat, J.-F., Pitman, A. J., Zhang, Q., Abramowitz, G. and Wang, Y.-P.: Examining soil
399 carbon uncertainty in a global model: response of microbial decomposition to temperature,
400 moisture and nutrient limitation, Biogeosciences, 10(11), 7095–7108, doi:10.5194/bg-10-7095-
401 2013, 2013b.

402 Exbrayat, J.-F., Pitman, A. J., and Abramowitz, G.: Disentangling residence time and
403 temperature sensitivity of microbial decomposition in a global soil carbon model,
404 Biogeosciences Discuss., 11, 4995-5021, doi:10.5194/bgd-11-4995-2014, 2014.

405 Falloon, P., Jones, C. D., Ades, M. and Paul, K.: Direct soil moisture controls of future global
406 soil carbon changes: An important source of uncertainty, Global Biogeochem. Cycles, 25,
407 GB3010, doi:201110.1029/2010GB003938, 2011.

408 FAO/IIASA/ISRIC/ISSCAS/JRC: Harmonized World Soil Database (version 1.21). FAO,
409 Rome, Italy and IIASA, Laxenburg, Austria, 2012.

410 Foley, J. A.: An equilibrium model of the terrestrial carbon budget, Tellus B, 47(3), 310–319,
411 doi:10.1034/j.1600-0889.47.issue3.3.x, 1995.

412 Friedlingstein, P., Meinshausen, M., Arora, V. K., Jones, C. D., Anav, A., Liddicoat, S. K. and
413 Knutti, R.: Uncertainties in CMIP5 Climate Projections due to Carbon Cycle Feedbacks, J.
414 Clim., 27(2), 511–526, doi:10.1175/JCLI-D-12-00579.1, 2014.

415 Friend, A. D., Lucht, W., Rademacher, T. T., Keribin, R., Betts, R., Cadule, P., Ciais, P., Clark,
416 D. B., Dankers, R., Falloon, P. D., Ito, A., Kahana, R., Kleidon, A., Lomas, M. R., Nishina, K.,
417 Ostberg, S., Pavlick, S., Peylin, P., Schaphoff, S., Vuichard, N., Warszawski, L., Wiltshire, A.,
418 and Woodward, F. I.:Carbon residence time dominates uncertainty in terrestrial vegetation 508
419 responses to future climate and atmospheric CO_2, Proc. Natl. Acad. Sci., 111(9), 3280-3285,
420 doi:10.1073/pnas.1222477110, 2014.

421 Gent, P. R., Danabasoglu, G., Donner, L. J., Holland, M. M., Hunke, E. C., Jayne, S. R.,
422 Lawrence, D. M., Neale, R. B., Rasch, P. J., Vertenstein, M., Worley, P. H., Yang, Z.-L. and
423 Zhang, M.: The Community Climate System Model Version 4, J. Clim., 24(19), 4973–4991,
424 doi:10.1175/2011JCLI4083.1, 2011.

425 Giorgetta, M. A., Jungclaus, J., Reick, C. H., Legutke, S., Bader, J., Böttinger, M., Brovkin, V.,
426 Crueger, T., Esch, M., Fieg, K., Glushak, K., Gayler, V., Haak, H., Hollweg, H.-D., Ilyina, T.,
427 Kinne, S., Kornblueh, L., Matei, D., Mauritsen, T., Mikolajewicz, U., Mueller, W., Notz, D.,
428 Pithan, F., Raddatz, T., Rast, S., Redler, R., Roeckner, E., Schmidt, H., Schnur, R.,
429 Segschneider, J., Six, K. D., Stockhause, M., Timmreck, C., Wegner, J., Widmann, H., Wieners,
430 K.-H., Claussen, M., Marotzke, J. and Stevens, B.: Climate and carbon cycle changes from 1850
431 to 2100 in MPI-ESM simulations for the Coupled Model Intercomparison Project phase 5, J.
432 Adv. Model. Earth Syst., 5(3), 572–597, doi:10.1002/jame.20038, 2013.

433 Hugelius, G., Tarnocai, C., Broll, G., Canadell, J. G., Kuhry, P., and Swanson, D. K.: The
434 Northern Circumpolar Soil Carbon Database: spatially distributed datasets of soil coverage and
435 soil carbon storage in the northern permafrost regions, Earth Syst. Sci. Data, 5, 3-13,
436 doi:10.5194/essd-5-3-2013, 2013.

Ito, A.: A historical meta-analysis of global terrestrial net primary productivity: are estimates converging? Glob. Change Biol., 17, 3161–3175, doi:10.1111/j.1365-2486.2011.02450.x, 2011.

Jenkinson, D. S.: The turnover of organic-carbon and nitrogen in soil, Philos. T. R. Soc. Lond., 329, 361–368, 1990.

Ji, J., Huang, M. and Li, K.: Prediction of carbon exchanges between China terrestrial ecosystem and atmosphere in 21st century, Sci. China Ser. D Earth Sci., 51(6), 885–898, doi:10.1007/s11430-008-0039-y, 2008.

Jobbágy, E. G. and Jackson, R. B.: The vertical distribution of soil organic carbon and its relation to climate and vegetation, Ecol. Appl., 10(2), 423–436, doi:10.1890/1051-0761(2000)010[0423:TVDOSO]2.0.CO;2, 2000.

Kirschbaum, M. U. F.: Soil respiration under prolonged soil warming: are rate reductions caused by acclimation or substrate loss?, Glob. Chang. Biol., 10(11), 1870–1877, doi:10.1111/j.1365-2486.2004.00852.x, 2004.

Knorr, W.: Annual and interannual CO2 exchanges of the terrestrial biosphere: process-based simulations and uncertainties, Glob. Ecol. Biogeogr., 9(3), 225–252, doi:10.1046/j.1365-2699.2000.00159.x, 2000.

Knorr, W., Prentice, I. C., House, J. I. and Holland, E. A.: Long-term sensitivity of soil carbon turnover to warming, Nature, 433(7023), 298–301, doi:10.1038/nature03226, 2005.

Krinner, G., Viovy, N., de Noblet-Ducoudré, N., Ogée, J., Polcher, J., Friedlingstein, P., Ciais, P., Sitch, S. and Prentice, I. C.: A dynamic global vegetation model for studies of the coupled atmosphere-biosphere system, Global Biogeochem. Cycles, 19(1), GB1015, doi:10.1029/2003GB002199, 2005.

Lawrence, D. M., Oleson, K. W., Flanner, M. G., Thornton, P. E., Swenson, S. C., Lawrence, P. J., Zeng, X., Yang, Z.-L., Levis, S., Sakaguchi, K., Bonan, G. B. and Slater, A. G.: Parameterization improvements and functional and structural advances in Version 4 of the Community Land Model, J. Adv. Model. Earth Syst., 3(3), M03001, doi:10.1029/2011MS000045, 2011.

Lloyd, J. and Taylor, J. A.: On the Temperature Dependence of Soil Respiration, Funct. Ecol., 8, 315–323, 1994.

Lund, M., Lafleur, P. M., Roulet, N. T., Lindroth, A., Christensen, T. R., Aurela, M., Chojnicki, B. H., Flanagan, L. B., Humphreys, E. R., Laurila, T., Oechel, W. C., Olejnik, J., Rinne, J.,

468 Schubert, P. and Nilsson, M. B.: Variability in exchange of CO2 across 12 northern peatland and
469 tundra sites, Glob. Chang. Biol., no–no, doi:10.1111/j.1365-2486.2009.02104.x, 2009.

470 Luo, Y., Wan, S., Hui, D. and Wallace, L. L.: Acclimatization of soil respiration to warming in a
471 tall grass prairie., Nature, 413(6856), 622–5, doi:10.1038/35098065, 2001.

472 Nishina, K., Ito, A., Beerling, D. J., Cadule, P., Ciais, P., Clark, D. B., Falloon, P., Friend, A. D.,
473 Kahana, R., Kato, E., Keribin, R., Lucht, W., Lomas, M., Rademacher, T. T., Pavlick, R.,
474 Schaphoff, S., Vuichard, N., Warszawaski, L. and Yokohata, T.: Quantifying uncertainties in
475 soil carbon responses to changes in global mean temperature and precipitation, Earth Syst. Dyn.,
476 5(1), 197–209, doi:10.5194/esd-5-197-2014, 2014.

477 Parton, W. J., Schimel, D. S., Cole, C. V. and Ojima, D. S.: Analysis of Factors Controlling Soil
478 Organic Matter Levels in Great Plains Grasslands1, Soil Sci. Soc. Am. J., 51(5), 1173-1179,
479 doi:10.2136/sssaj1987.03615995005100050015x, 1987.

480 Parton, W. J., Stewart, J. W. B. and Cole, C. V.: Dynamics of C, N, P and S in grassland soils: a
481 model, Biogeochemistry, 5(1), 109–131, doi:10.1007/BF02180320, 1988.

482 Le Quéré, C., Raupach, M. R., Canadell, J. G., Marland, G., Bopp, L., Ciais, P., Conway, T. J.,
483 Doney, S. C., Feely, R. A., Foster, P., Friedlingstein, P., Gurney, K., Houghton, R. A., House, J.
484 I., Huntingford, C., Levy, P. E., Lomas, M. R., Majkut, J., Metzl, N., Ometto, J. P., Peters, G. P.,
485 Prentice, I. C., Randerson, J. T., Running, S. W., Sarmiento, J. L., Schuster, U., Sitch, S.,
486 Takahashi, T., Viovy, N., van der Werf, G. R. and Woodward, F. I.: Trends in the sources and
487 sinks of carbon dioxide, Nat. Geosci., 2(12), 831–836, doi:10.1038/ngeo689, 2009.

488 Raddatz, T. J., Reick, C. H., Knorr, W., Kattge, J., Roeckner, E., Schnur, R., Schnitzler, K.-G.,
489 Wetzel, P. and Jungclaus, J.: Will the tropical land biosphere dominate the climate–carbon cycle
490 feedback during the twenty-first century?, Clim. Dyn., 29(6), 565–574, doi:10.1007/s00382-007-
491 0247-8, 2007.

492 Randerson, J. T., Thompson, M. V., Conway, T. J., Fung, I. Y. and Field, C. B.: The
493 contribution of terrestrial sources and sinks to trends in the seasonal cycle of atmospheric carbon
494 dioxide, Global Biogeochem. Cycles, 11(4), 535–560, doi:10.1029/97GB02268, 1997.

495 Sato, H., Itoh, A. and Kohyama, T.: SEIB–DGVM: A new Dynamic Global Vegetation Model
496 using a spatially explicit individual-based approach, Ecol. Modell., 200(3-4), 279–307,
497 doi:10.1016/j.ecolmodel.2006.09.006, 2007.

Schmidt, M. W. I., Torn, M. S., Abiven, S., Dittmar, T., Guggenberger, G., Janssens, I. A., Kleber, M., Kögel-Knabner, I., Lehmann, J., Manning, D. A. C., Nannipieri, P., Rasse, D. P., Weiner, S. and Trumbore, S. E.: Persistence of soil organic matter as an ecosystem property., Nature, 478(7367), 49–56, doi:10.1038/nature10386, 2011.

Shangguan, W., Dai, Y., Duan, Q., Liu, B., Yuan, H.: A global soil data set for earth system modeling, J. Adv. Model. Earth Syst., 6, 249–263, doi:10.1002/2013MS000293, 2014.

Shevliakova, E., Pacala, S. W., Malyshev, S., Hurtt, G. C., Milly, P. C. D., Caspersen, J. P., Sentman, L. T., Fisk, J. P., Wirth, C. and Crevoisier, C.: Carbon cycling under 300 years of land use change: Importance of the secondary vegetation sink, Global Biogeochem. Cycles, 23(2), GB2022, doi:10.1029/2007GB003176, 2009.

Shindell, D. T., Pechony, O., Voulgarakis, A., Faluvegi, G., Nazarenko, L., Lamarque, J.-F., Bowman, K., Milly, G., Kovari, B., Ruedy, R. and Schmidt, G. A.: Interactive ozone and methane chemistry in GISS-E2 historical and future climate simulations, Atmos. Chem. Phys., 13(5), 2653–2689, doi:10.5194/acp-13-2653-2013, 2013.

Taylor, K. E., Stouffer, R. J. and Meehl, G. A.: An overview of CMIP5 and the experiment design, Bull. Am. Meteorol. Soc., 93(4), 485–498, doi:10.1175/BAMS-D-11-00094.1, 2012.

Thornton, P. E., Lamarque, J.-F., Rosenbloom, N. A. and Mahowald, N. M.: Influence of carbon-nitrogen cycle coupling on land model response to CO 2 fertilization and climate variability, Global Biogeochem. Cycles, 21(4), GB4018, doi:10.1029/2006GB002868, 2007.

Thornton, P. E. and Rosenbloom, N. A.: Ecosystem model spin-up: Estimating steady state conditions in a coupled terrestrial carbon and nitrogen cycle model, Ecol. Modell., 189(1-2), 25–48, doi:10.1016/j.ecolmodel.2005.04.008, 2005.

Todd-Brown, K. E. O., Randerson, J. T., Post, W. M., Hoffman, F. M., Tarnocai, C., Schuur, E. a. G. and Allison, S. D.: Causes of variation in soil carbon simulations from CMIP5 Earth system models and comparison with observations, Biogeosciences, 10(3), 1717–1736, doi:10.5194/bg-10-1717-2013, 2013.

Warszawski, L., Frieler, K., Huber, V., Piontek, F., Serdeczny, O. and Schewe, J.: The Inter-Sectoral Impact Model Intercomparison Project (ISI-MIP): project framework., Proc. Natl. Acad. Sci. U. S. A., 111(9), 3228–32, doi:10.1073/pnas.1312330110, 2014.

Watanabe, S., Hajima, T., Sudo, K., Nagashima, T., Takemura, T., Okajima, H., Nozawa, T., Kawase, H., Abe, M., Yokohata, T., Ise, T., Sato, H., Kato, E., Takata, K., Emori, S. and

529 Kawamiya, M.: MIROC-ESM 2010: model description and basic results of CMIP5-20c3m
530 experiments, Geosci. Model Dev., 4(4), 845–872, doi:10.5194/gmd-4-845-2011, 2011.

531 Wieder, W. R., Bonan, G. B. and Allison, S. D.: Global soil carbon projections are improved by
532 modelling microbial processes, Nat. Clim. Chang., 3(10), 909–912, doi:10.1038/nclimate1951,
533 2013.

534 Wu, T., Li, W., Ji, J., Xin, X., Li, L., Wang, Z., Zhang, Y., Li, J., Zhang, F., Wei, M., Shi, X.,
535 Wu, F., Zhang, L., Chu, M., Jie, W., Liu, Y., Wang, F., Liu, X., Li, Q., Dong, M., Liang, X.,
536 Gao, Y. and Zhang, J.: Global carbon budgets simulated by the Beijing Climate Center Climate
537 System Model for the last century, J. Geophys. Res. Atmos., 118(10), 4326–4347,
538 doi:10.1002/jgrd.50320, 2013.

539 Xenakis, G. and Williams, M.: Comparing microbial and chemical kinetics for modelling soil
540 organic carbon decomposition using the DecoChem v1.0 and DecoBio v1.0 models, Geosci.
541 Model Dev., 7, 1519-1533, doi:10.5194/gmd-7-1519-2014, 2014.

542 Xia, J., Luo, Y., Wang, Y.-P. and Hararuk, O.: Traceable components of terrestrial carbon
543 storage capacity in biogeochemical models., Glob. Chang. Biol., 19(7), 2104–16,
544 doi:10.1111/gcb.12172, 2013.

545 Xia, J. Y., Luo, Y. Q., Wang, Y.-P., Weng, E. S. and Hararuk, O.: A semi-analytical solution to
546 accelerate spin-up of a coupled carbon and nitrogen land model to steady state, Geosci. Model
547 Dev., 5(5), 1259–1271, doi:10.5194/gmd-5-1259-2012, 2012.

548

549

Tables

Table 1. CMIP5 models and number of simulations used in this paper for historical and RCP 8.5 runs. The first column provides the letter code used in the figures. References and details about soil carbon components are provided in supplementary Tables 2 and 3.

	Model name	Institution	Number of model runs	
			Historical	RCP 8.5
A	BCC-CSM1.1	Beijing Climate Center (China)	3	0
B	CanESM2	Canadian Centre for Climate Modelling and Analysis (Canada)	5	5
C	CCSM4	National Center for Atmospheric Research (USA)	6	6
D	GFDL-ESM2G	Geophysical Fluid Dynamics Laboratory (USA)	1	1
E[a]	GISS-E2-H	NASA Goddard Institute for Space Studies (USA)	17	3
	GISS-E2-R		25	3
F[a]	HadGEM2-CC	Met Office/Hadley Centre (UK)	1	1
	HadGEM2-ES		3	3
G[a]	IPSL-CM5A-LR	Institut Pierre Simon Laplace (France)	6	4
	IPSL-CM5B-LR		1	1
H[a]	MIROC-ESM	Japan Agency for Marine-Earth Science and Technology (Japan)	3	1
	MIROC-ESM-CHEM		1	1
I	MPI-ESM-LR	Max Planck Institute (Germany)	3	3
J[a]	NorESM1-M	Bjerknes Centre for Climate Research (Norway)	3	1
	NorESM1-ME		1	1

[a]models from the same institution where averaged to avoid pseudo-replication

555 **Table 2.** Details about the CMIP5 models terrestrial and soil component and associated references.

	Model name	Terrestrial component	Soil biogeochemistry	# of pools		N limitations
				L	S	
A	BCC-CSM1.1 (Wu et al., 2013)	AVIM2 (Ji et al., 2008)	Based on CENTURY (Parton et al., 1987)	2	6	Yes
B	CanESM2 (Chylek et al., 2011)	CTEM (Arora and Boer, 2010)	CTEM (Arora and Boer, 2010)	1	1	No
C	CCSM4 (Gent et al., 2011)	CLM4-CN (Lawrence et al., 2011)	CN module (Thornton et al., 2007) based on Biome-BGC 4.1.2 (Thornton and Rosenbloom, 2005)	3	3	Yes
D	GFDL-ESM2G (Dunne et al., 2012)	LM3.0 (Shevliakova et al., 2009)	Based on CENTURY (Parton et al., 1987)	–	2	No
E	GISS-E2 (Shindell et al., 2013)	NCAR-CSM1.4 (Doney et al., 2006)	Based on CASA (Randerson et al., 1997)	–	9	No
F	HadGEM2 (Collins et al., 2011)	JULES (Clark et al., 2011)	Based on TRIFFID (Cox, 2001) and RothC (Jenkinson, 1990)	–	4	No
G	IPSL-CM5 (Dufresne et al., 2013)	ORCHIDEE	STOMATE (Krinner et al., 2005) and CENTURY (Parton et al., 1988)	3	4	No
H	MIROC-ESM (Watanabe et al., 2011)	SEIB-DGVM (Sato et al., 2007)	Based on DEMETER-1 (Foley et al., 2005)	–	2	No
I	MPI-ESM-LR (Giorgetta et al., 2013)	JSBACH (Raddatz et al., 2007)	Based on Bethy (Knorr, 2000) and CENTURY (Parton et al., 1988)	1	1	No

J	NorESM1 (Bentsen et al., 2012)	CLM4-CN (Lawrence et al., 2011)	CN module (Thornton et al., 2007) based on Biome-BGC 4.1.2 (Thornton and Rosenbloom, 2005)	3	3	Yes

Table 3. Model specific values of SOC_{in}, R_h and SOC used in Figures 1 to 4. Values are averaged over the indicated years. All data are rounded to whole numbers. Values for 2091-2100 are from the Representative Concentration Pathway 8.5 (RCP 8.5) simulations.

Model	SOC_{in} [Pg C yr^{-1}]			R_h [Pg C yr^{-1}]			Total soil carbon [Pg C]		
	1861-1870	1996-2005	2091-2100	1861-1870	1996-2005	2091-2100	1861-1870	1996-2005	2091-2100
A	75	87	–	75	86	–	1273	1351	–
B	57	64	84	56	65	85	1511	1541	1490
C	46	49	56	46	49	57	563	576	582
D	79	85	119	79	86	120	1798	1781	1785
E	45	55	58	45	55	61	2113	2306	2118
F	67	86	140	67	84	137	1178	1287	1596
G	76	87	123	76	87	123	1598	1626	1709
H	57	59	71	56	55	74	2515	2566	2494
I	66	75	100	66	74	99	2938	3047	3266
J	52	55	61	52	55	62	650	666	654

560 **Figure legends**

561 **Figure 1.** Relationship between total *SOC* in CMIP5 models at two different times: modern
562 stocks as a function of pre-industrial stocks (upper panel), future stocks as a function of
563 modern stocks (middle panel) and future stocks as a function of pre-industrial stocks (lower
564 panel). Letters correspond to models as in Table 1 and models in green (i.e. C and J) integrate
565 nitrogen limitation. The gray area is the 95% confidence interval of modern total *SOC* derived
566 from the HWSD. Equation, R^2 and p values correspond to the linear relationship between
567 stocks built using data from all models (solid line). The dotted line is the 1:1 line.
568
569 **Figure 2.** Relationship between pre-industrial global *SOC* input and pre-industrial R_h. Letters
570 are the same as in Table 1 and models in green (i.e. C and J) integrate nitrogen limitation. The
571 solid line is a linear relationship constructed using all models with equation, R^2 and p values
572 indicated in the top left corner. The dashed line represents the 1:1 relationship.
573
574 **Figure 3.** Relationship between pre-industrial *SOC* input and pre-industrial total *SOC* stocks
575 at the beginning of the historical experiment. Letters correspond to the same models as in
576 Table 1 and models in green (i.e. C and J) integrate nitrogen limitation. The solid line is a
577 linear relationship constructed using all models with equation, R^2 and p values indicated in
578 the top left corner.
579
580 **Figure 4.** Relationship between pre-industrial global *SOC* turnover time and total *SOC*.
581 Letters correspond to the same models as in Table 1 and models in green (i.e. C and J)
582 integrate nitrogen limitation. The solid line is a linear relationship constructed using all
583 models with equation, R^2 and p values indicated in the top left corner.
584

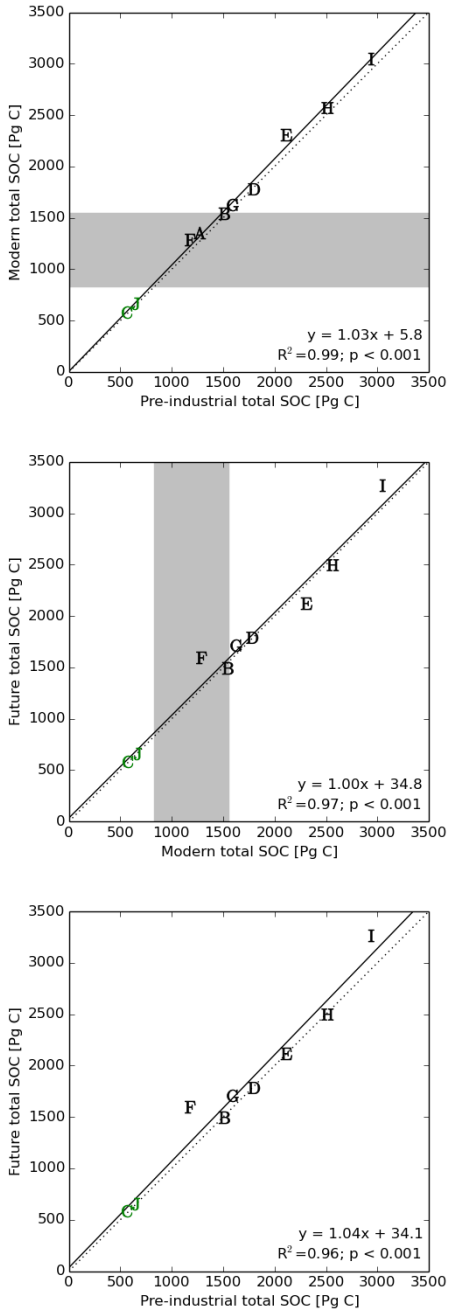

585

586 **Figure 1.** Relationship between total *SOC* in CMIP5 models at two different times: modern
587 stocks as a function of pre-industrial stocks (upper panel), future stocks as a function of
588 modern stocks (middle panel) and future stocks as a function of pre-industrial stocks (lower
589 panel). Letters correspond to models as in Table 1 and models in green (i.e. C and J) integrate
590 nitrogen limitation. The gray area is the 95% confidence interval of modern total *SOC* derived
591 from the HWSD. Equation, R^2 and p values correspond to the linear relationship between
592 stocks built using data from all models (solid line). The dotted line is the 1:1 line.

593

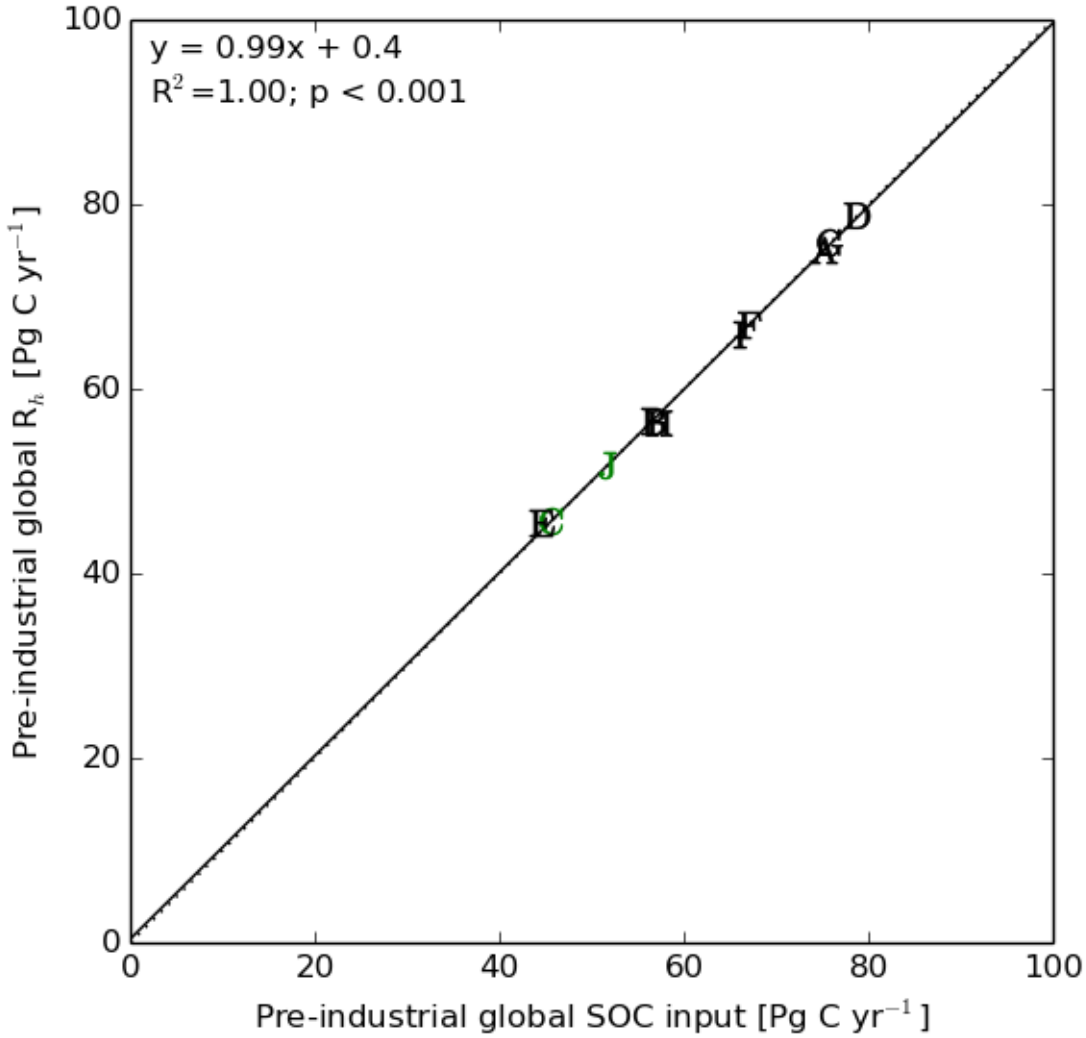

Figure 2. Relationship between pre-industrial global *SOC* input and pre-industrial R_h. Letters are the same as in Table 1 and models in green (i.e. C and J) integrate nitrogen limitation. The solid line is a linear relationship constructed using all models with equation, R^2 and p values indicated in the top left corner. The dashed line represents the 1:1 relationship.

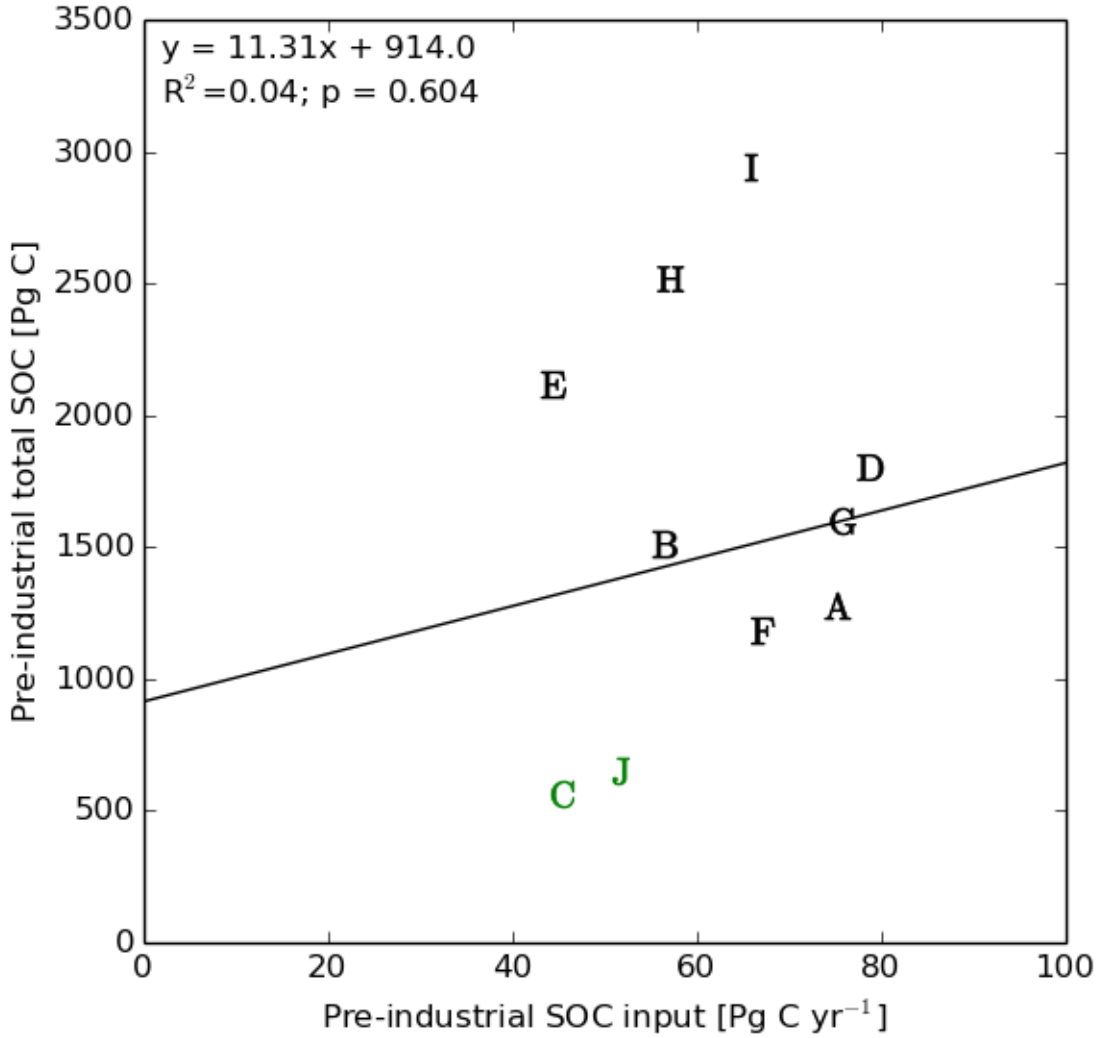

Figure 3. Relationship between pre-industrial *SOC* input and pre-industrial total *SOC* stocks at the beginning of the historical experiment. Letters correspond to the same models as in Table 1 and models in green (i.e. C and J) integrate nitrogen limitation. The solid line is a linear relationship constructed using all models with equation, R^2 and p values indicated in the top left corner.

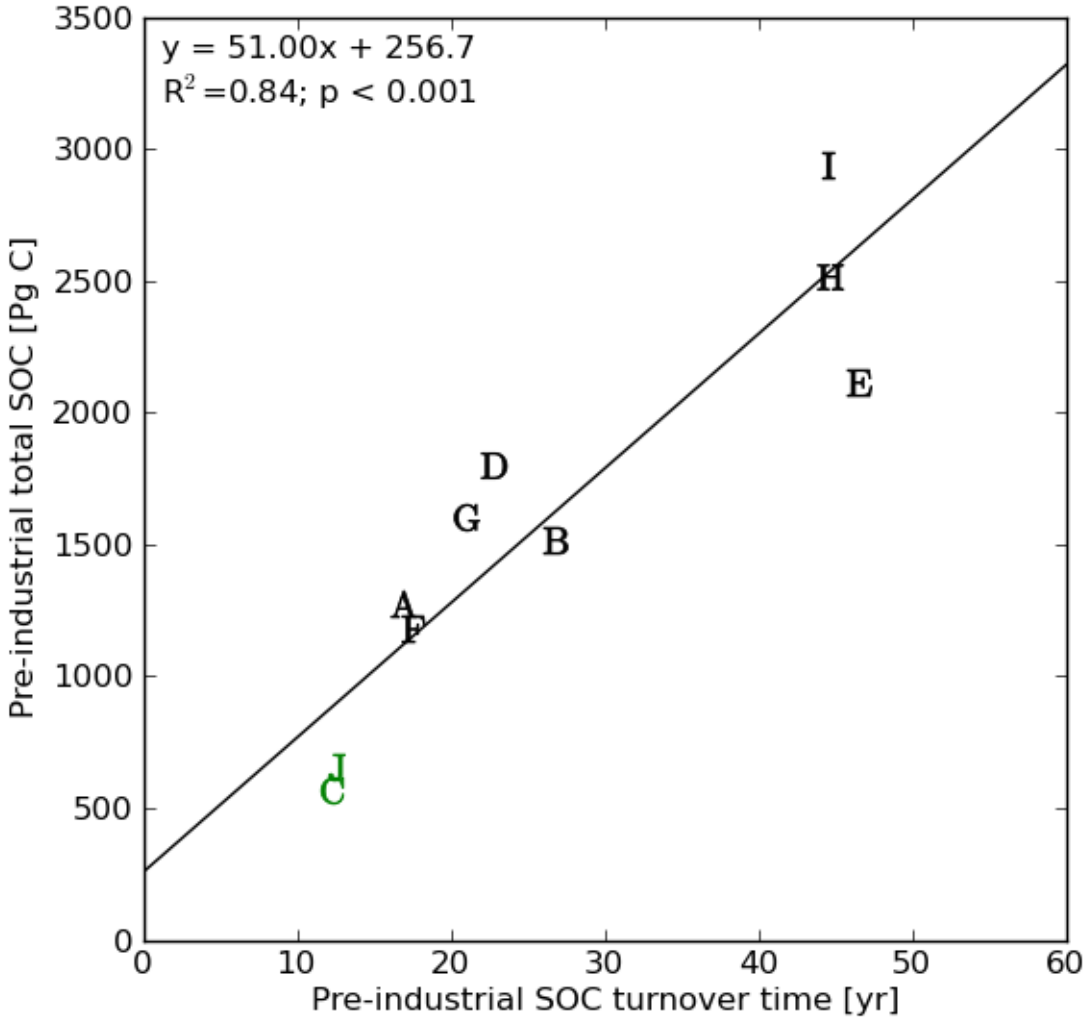

Figure 4. Relationship between pre-industrial global *SOC* residence time and total *SOC*. Letters correspond to the same models as in Table 1 and models in green (i.e. C and J) integrate nitrogen limitation. The solid line is a linear relationship constructed using all models with equation, R^2 and p values indicated in the top left corner.